Article

J. Mex. Chem. Soc. **2010**, *54(4),* 216-222

ISSN 1870-249X

Kinetic Modeling of the Alkaline Decomposition and Cyanidation of Argentojarosite

Francisco Patiño,[1]* Antonio Roca,[2] Martín Reyes,[1] Montserrat Cruells,[2] Isauro Rivera[1] and Leticia Esperanza Hernández[1]

[1] Centro de Investigaciones en Materiales y Metalurgia, Universidad Autónoma del Estado de Hidalgo, Carretera Pachuca-Tulancingo km 4.5, C.P. 42184, Pachuca, Hidalgo, México. Tel: 017717172000-ext 2282, e-mail: franpac@infosel.net.mx

[2] Departament de Ciència dels Materials i Enginyería Metallúrgica de Barcelona, Martí i Franquès 1, Barcelona, E-08028, España.

Received June 9, 2010; accepted September 6, 2010

Abstract. The jarosite sample used is an argentojarosite-hydroniumjarosite solid solution of approximate formula $(Ag_{0.78}H_3O_{0.22})Fe_3(SO_4)_2(OH)_6$. The decomposition process in $NaOH/Ca(OH)_2$ media and the cyanidation process in $Ca(OH)_2$ media were studied for the induction period and progressive conversion period respectively, and the reaction order and activation energy were determined for each case. The results are consistent with the spherical particle shrinking core model and chemical control under the experimental conditions imposed; six partial models and three global models have been tested for both processes in their basic behaviour.
Keywords: Argentojarosite, alkaline decomposition, kinetics, model, induction period, reaction order, activation energy.

Resumen. El producto utilizado es una solución sólida de argentojarosita-hidroniojarosita de fórmula aproximada $(Ag_{0.78}H_3O_{0.22})Fe_3(SO_4)_2(OH)_6$. Se estudió el proceso de descomposición en medio $NaOH/Ca(OH)_2$ y el proceso de cianuración en medio $Ca(OH)_2$ para el período de inducción y el de conversión progresiva, respectivamente, determinándose para cada caso el orden de reacción y la energía de activación. Los resultados son consistentes con el modelo de partícula esférica con núcleo decreciente y control químico en las condiciones experimentalmente empleadas; para ambos procesos se desarrollaron seis modelos parciales y tres modelos globales para describir su comportamiento básico.
Palabras clave: Argentojarosita, descomposición alcalina, cinética, modelo, período de inducción, orden de reacción, energía de activación.

Introduction

Although nine jarosite-type compounds have been synthesized, only six of them have been found in nature [1]. All of the known members of the jarosite family compounds are represented by the general formula $MFe_3(SO_4)_2(OH)_6$, where M^+ is H_3O^+, Na^+, K^+, Rb^+, Ag^+, NH_4^+, Tl^+, $1/2Pb^{2+}$ and $1/2Hg^{2+}$.

Jarosite-type minerals, mainly argentojarosite and plumbojarosite have a long history as sources of silver and/or lead. Man has been involved with these minerals since around 1200 B.C., when, at Río Tinto, Spain, jarosite-type minerals rich in Pb and Ag were extracted [2]. The silver of that deposit has been found as: a) argentojarosite, b) as solid solution in other jarosites, c) as argentite, and d) as cerargirite [1, 3]. It is known that before the Spanish arrived in the Americas, the Incas processed rich argentian plumbojarosite deposits located in the mine of Matagente, Peru. Such metallurgical operations were widespread among the Americas' pre-Columbian civilizations [4]. At the beginning of the 20th century, the Tintic Standard Mining Company at Dividend, Utah [5] located an important argentojarosite deposit with values of 8 to 34 kg of silver per ton of mineral.

Another source of argentian jarosite compounds comes from large-scale artificial processes. In this regard, in the 1970s and 1980s important efforts were made to incorporate the jarosite precipitation in the hydrometallurgical circuits as a way to eliminate iron and other impurities, to control sulfates and to considerably improve the filtering process. The industrial application of this technology appeared first in the film industry [4, 6], and because of the success of the use of jarosite precipitation in the hydrometallurgical circuits of more than 60 film plants [6], its application was spread to the hydrometallurgy of other metals, such as copper and cobalt [5]. The jarosite precipitation process solves some problems, like the ones already cited, but generates Zn and Ag losses in the jarositic residuals [7], which also means considerable losses from an economic point of view, mainly of silver.

This work is based on the study of decomposition and cyanidation in alkaline media of argentojarosite [8, 9]. For this reason, a comparison of rates and dependences was carried out in a wide range of experimental conditions relating concentration, temperature and particle size, as well as the reaction's stoichiometry and development of the partial and global kinetic models of the induction, decomposition and cyanidation periods of the argentojarosite in NaOH and $Ca(OH)_2$ media.

Results and discussion

Topology of the reaction

The decomposition and cyanidation of the argentojarosite in NaOH and $Ca(OH)_2$ media presents an induction period (θ), during which the jarosite does not react, and therefore the $SO_4^=$ and Ag^+ concentration in the solution are negligible (Figure 2). The induction period has been observed in the

Fig. 1. Image of the crystalline aggregates of particle size 36-40 µm used for the modeling process. SEM.

decomposition of jarosites synthesized in the laboratory and of jarosites coming from the industrial plant [13]. The concatenation of ions of the media on the particle surface causes the creation of active sites until a reaction front is established, by which both the media ions and the argentojarosite ions will start to diffuse, giving rise to a progressive conversion period, where the $SO_4^{=}$ and Ag^+ concentrations in the solution increase in a progressive manner until the sulfate and silver ion concentrations are stabilized (Figure 2), which means that the reaction has concluded. Figure 3 is a Scanning Electron Microscopy (SEM) image of an argentojarosite particle, showing an unreacted jarosite core surrounded by a reaction front, which is followed by an amorphous gel of iron and silver hydroxides. This gel can evolve and give rise to a crystalline silver ferrite, as seen on the X-ray spectra of Figure 4 of the alkaline reactivity of the argentojarosite at different times up to the total decomposition (from 0 to 4 hours) according to the following process [9]:

$$AgFe_3(SO_4)_2(OH)_{6(s)} + 4OH^-_{(aq)} \rightarrow Ag(OH)_{(s)} + 3Fe(OH)_{3(s)} + 2SO_4^{2-}{}_{(aq)} \quad (1)$$

$$Ag(OH)_{(s)} + Fe(OH)_{3(s)} \rightarrow \tfrac{1}{2}\, Ag_2O{\cdot}Fe_2O_{3(s)} + 2H_2O \quad (2)$$

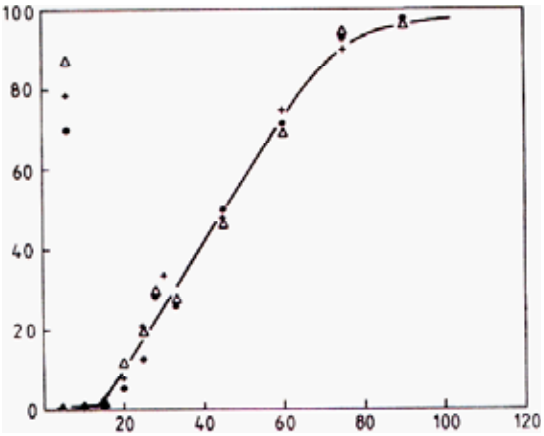

Fig. 2. Decomposition and cyanidation curve of the argentojarosite. pH 12, 36-40 µm and 30 ºC.

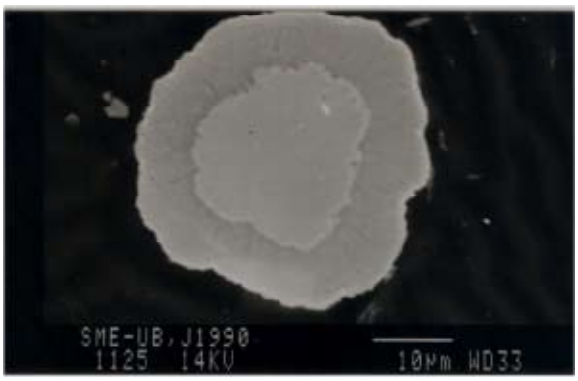

Fig. 3. Backscattered electron image of an argentojarosite particle, partially decomposed with NaOH, pH 12 and 30 ºC.

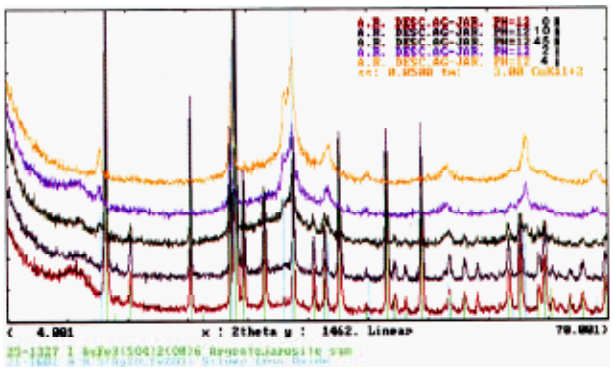

Fig. 4. X-ray diffraction diagram of the alkaline decomposition solids at different times: 30 ºC, pH 12 and 40-56 µm.

Partial decomposition of the silver ferrite to metallic silver has been observed at temperatures over 100 ºC, as observed in the X-ray spectrum of Figure 5a, while decomposition is total at 600ºC. At that temperature the iron is found as crystalline Fe_2O_3, as observed in Figure 5b. The process can be represented by:

$$AgO{\cdot}Fe_2O_{3(s)} \rightarrow Fe_2O_{3(s)} + 2Ag_{(s)} + 1/2O_{2(s)} \quad (3)$$

Cyanidation of the decomposition products of the argentojarosite can be described through the complexation of the reaction products of equation 1:

$$Ag(OH)_{(s)} + 2CN^-_{(aq)} \rightarrow Ag(CN)^-_{2(aq)} + OH^-_{(aq)} \quad (4)$$

All the experimental results of the decomposition and cyanidation of the argentojarosite in NaOH and $Ca(OH)_2$ media are consistent with the shrinking core kinetic model for constant-size spherical particles, where the process is controlled by the chemical reaction step [14, 15, 16]:

$$k_{exp}t = 1 - (1 - X)^{1/3} \quad (5)$$

In which,

$$k_{exp} = V_M k_q c^n{}_A / r_0 \quad (6)$$

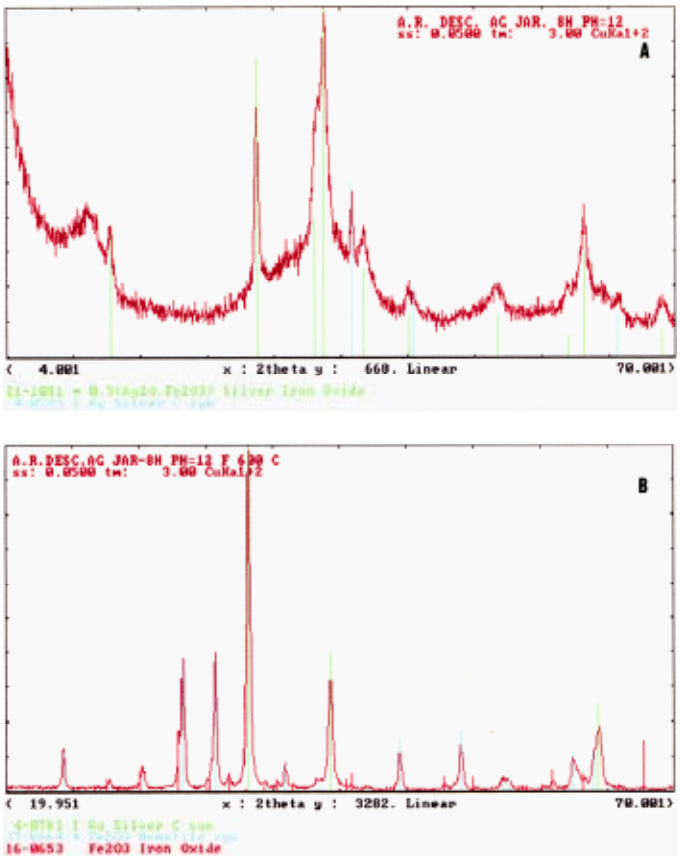

Fig. 5. A: Spectrum of a total decomposition product in NaOH media heated at 110 °C during 3h. B: Id. Calcinated at 600 °C during 2h.

Where k_{exp} is the experimental rate constant, X is the reacted fraction, V_M is the solid's molar volume, c_A is the reactant concentration, r_0 is the particle's initial radius, k_q is the rate constant of the chemical reaction and n is the order of the reaction. Note in Figure 6 that the experimental results shown in Figure 2 are consistent with the chemical control expression as the rate-controlling stage.

Modeling

Argentojarosite decomposition in alkaline media

Tables 1, 2, 3 and 4 summarize the experimental results, where the induction periods (θ) and experimental rate constants are presented for a wide range of experimental conditions of concentration (NaOH, $Ca(OH)_2$ and NaCN), temperature and particle size. For the decomposition of the argentojarosite in NaOH and $Ca(OH)_2$ < 2mM media corresponding to the induction period a fractional reaction order of n = 0.5 is obtained, with an activation energy of E_a = 71 kJ mol^{-1}. According to these results, the induction period is defined by the expression:

$$1/\theta = [OH]^{0.5} \cdot 7.4 \cdot 10^{11} \cdot e^{-71{,}000/RT} \quad (7)$$

For the decomposition corresponding to the progressive conversion period under the alkaline concentration conditions

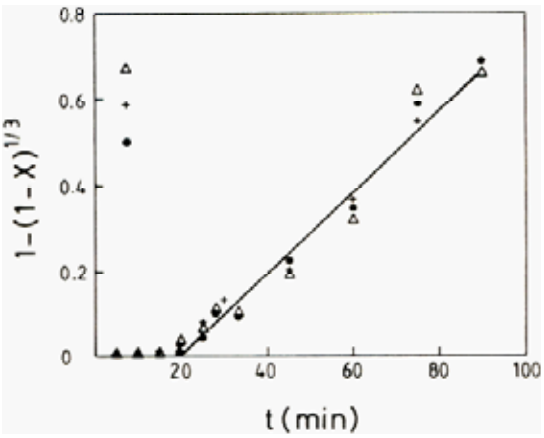

Fig. 6. Representation of the shrinking core model and chemical control for the data in Figure 2.

cited above, a fractional reaction order of n = 0.5 is obtained, with an activation energy of E_a = 42 kJ mol^{-1}. Therefore, the kinetic expression for the progressive conversion period is:

$$(r_0/V_M)\,[1-(1-X)^{1/3}] = 59.1 \cdot e^{-42{,}000/RT} \cdot [OH]^{0.5} \cdot t \quad (8)$$

Figure 7 shows the performance of the kinetic model of Equation 7, plotting the experimental induction time, $\theta_{(experimental)}$ (min) vs induction time, $\theta_{(model)}$ (min). In the same way, Figure 8 presents the performance of the model of equation 8, plotting the experimental rate constant, k_{exp} (min^{-1}) vs the model rate constant, $k_{exp,\,(model)}$ (min^{-1}).

In the case of the decomposition of argentojarosite in $Ca(OH)_2$ > 2mM media a reaction order of n = 0 is obtained for the induction period, with an activation energy of E_a=71 kJ mol^{-1}; the expression for the induction period is the following:

$$1/\theta = [OH]^0 \cdot 3.6 \cdot 10^{10} \cdot e^{-71{,}000/RT} \quad (9)$$

Just as above, according to the shrinking core model and chemical control a reaction order of n = 0 with activation energy of E_a = 42 kJ mol^{-1} is obtained for the progressive conversion period; the expression for this period is defined as:

$$(r_0/V_M)\,[1-(1-X)^{1/3}] = 2.34 \cdot e^{-42{,}000/RT} \cdot [OH]^0 \cdot t \quad (10)$$

Figure 9 shows the comparison $\theta_{(model)}$ vs $\theta_{(experimental)}$; Figure 10 compares $k_{exp(calculated)}$ vs $k_{exp(experimental)}$, including, in both cases, all of the experimental data obtained. Therefore, equations 9 and 10 describe well the experimental results.

Cyanidation of argentojarosite

The cyanidation of the argentojarosite in $Ca(OH)_2$ > 2mM media corresponding to the induction period yields an activation energy of E_a = 71.0 kJ mol^{-1}, with a reaction order of n = 0.5. According to these results, the kinetic expression for the induction period is:

$$1/\theta = [CN^-]^{0.5} \cdot 3.0 \cdot 10^6 \cdot e^{-71{,}000/RT} \quad (11)$$

Table 1. Argentojarosite decomposition in NaOH media: $n = 0.5$ and $E_a = 42$ KJ mol^{-1}. For the induction period $n = 0.5$ and $E_a = 71$ kJ mol^{-1}.

pH	[OH$^-$]	TºC	Particle diameter (μm)	Induction time, θ (min)	k_{exp} (min^{-1})
12.25	0.02600	30	48.0	9.0	2.1×10^{-2}
11.88	0.01100	30	48.0	29.0	1.12×10^{-2}
11.30	0.00300	30	48.0	69.0	0.573×10^{-2}
10.62	0.00062	30	48.0	12.70	0.335×10^{-2}
11.72	0.03000	50	48.0	1.00	7.460×10^{-2}
11.56	0.02000	50	48.0	0.10	6.000×10^{-2}
11.13	0.00740	50	48.0	5.00	3.260×10^{-2}
10.70	0.00280	50	48.0	16.00	1.930×10^{-2}
10.30	0.00110	50	48.0	20.00	1.370×10^{-2}
9.40	0.00014	50	48.0	45.00	0.346×10^{-2}
11.00	0.00950	60	48.0	—	3.780×10^{-2}
10.47	0.00280	60	48.0	2	2.210×10^{-2}
10.10	0.00120	60	48.0	9	1.640×10^{-2}
17.00	9.5×10^{-7}	60	48.0	18	4.500×10^{-4}
12.00	0.0100	23	48.0	48	0.977×10^{-2}
11.64	0.0091	35	48.0	14	1.680×10^{-2}
11.54	0.0100	40	48.0	7	1.810×10^{-2}
11.88	0.0110	30	30.5	30	1.600×10^{-2}
11.88	0.0110	30	38.0	26	1.300×10^{-2}
11.88	0.0110	30	59.5	27	0.836×10^{-2}
11.88	0.0110	30	71.5	16	0.653×10^{-2}

Table 2. Argentojarosite decomposition in $Ca(OH)_2$ media: $n = 0.5$ and $E_a = 42.00$ kJ mol^{-1}. For the induction period: $n = 0.5$ and $E_a = 71$ kJ mol^{-1}.

pH	[OH$^-$]	TºC	Particle diameter (μm)	Induction time, θ (min)	k_{exp} (min^{-1})
10.44	0.00150	50	38	10.0	1.22×10^{-2}
10.14	0.00076	50	38	14.5	0.828×10^{-2}
9.61	0.00025	50	38	25.0	0.455×10^{-2}

Table 3. Argentojarosite decomposition in $Ca(OH)_2$ media: $n = 0$ and $E_a = 42$ kJ mol^{-1}. For the induction period: $n = 0$ and $E_a = 71$ kJ mol^{-1}.

pH	[OH$^-$]	TºC	Particle diameter (μm)	Induction time, θ (min)	k_{exp} (min^{-1})
11.88	0.04170	50	38	8.0	1.40×10^{-2}
11.46	0.01580	50	38	11.5	1.72×10^{-2}
11.35	0.01230	50	38	9.0	1.36×10^{-2}
10.99	0.00054	50	38	14.0	1.88×10^{-2}
12.14	0.02030	30	38	43.0	0.459×10^{-2}
12.00	0.02920	40	38	22.0	0.929×10^{-2}
11.70	0.04790	60	38	3.7	1.99×10^{-2}
11.46	0.01580	50	30.5	12.0	2.14×10^{-2}
11.46	0.01580	50	59.5	10.0	1.13×10^{-2}
11.46	0.01580	50	90.0	4.0	0.977×10^{-2}

Table 4. Argentojarosite cyanidation in $Ca(OH)_2$ media: $n = 0$ and $E_a = 42$ kJ mol^{-1}. For the induction period: $n = 0.5$ and $E_a = 71$ kJ mol^{-1}.

pH	[OH$^-$]	TºC	Particle diameter (μm)	Induction time, θ (min)	k_{exp} (min^{-1})
11.64	0.024	50	38	9	1.91×10^{-2}
11.67	0.026	50	38	12	1.86×10^{-2}
11.69	0.027	50	38	23	1.74×10^{-2}
11.22	0.025	30	38	86	0.61×10^{-2}
12.15	0.029	35	38	67	0.85×10^{-2}
12.01	0.029	40	38	25	1.83×10^{-2}
11.80	0.025	45	38	21	1.60×10^{-2}

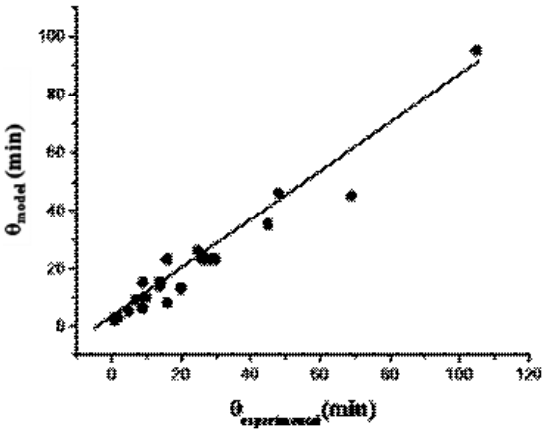

Fig. 7. Induction period for the alkaline decomposition: Comparison between calculated data and experimental data for θ. NaOH and $Ca(OH)_2 < 2$mM.

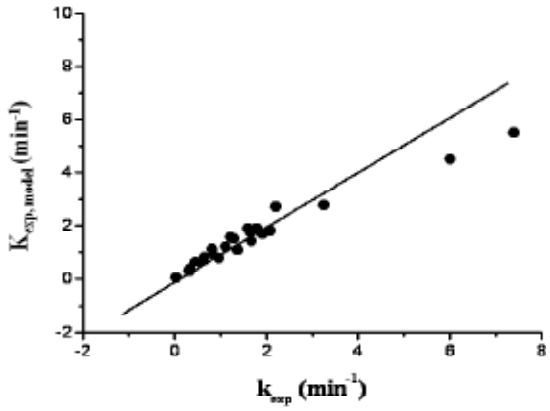

Fig. 8. Conversion period of the alkaline decomposition: Comparison between calculated data and experimental data for k_{exp}. NaOH and $Ca(OH)_2 < 2$mM.

For the progressive conversion period in $Ca(OH)_2 > 2$mM media an activation energy of E_a = 42 kJ mol^{-1} is obtained, with a reaction order of n = 0 for both [OH$^-$] and [CN$^-$]; therefore, the kinetic expression is:

$$(r_0/V_M)\,[1 - (1 - x)^{1/3}] = 59.1 \cdot e^{-42{,}000/RT} \cdot [OH]^0 \cdot [CN^-]^0 t \qquad (12)$$

In all the kinetic expressions V_M = 161.3 cm^3/mol; R = 8.31 J mol^{-1} K^{-1}; r_0 in cm; T in Kelvin; [OH$^-$] and [CN$^-$] in moles per liter; t in minutes.

Figure 11 is the induction time plot, showing $\theta_{(model)}$ against the experimental induction time $\theta_{(experimental)}$. Since equation 12 is basically identical to equation 10, Figure 10 is obtained after plotting $k_{exp(calculated)}$ vs $k_{exp(experimental)}$. Therefore we can conclude that expressions 11 and 12 are in good agreement with the experimental results.

Global models

Alkaline decomposition (NaOH and $Ca(OH)_2 < 2$mM).

For expressions 7 and 8 corresponding to the alkaline decomposition (NaOH and $Ca(OH)_2 < 2$mM), a general expression can be established in order to determine the total reaction time for obtaining a definite conversion of the argentojarosite; the kinetic model is the following:

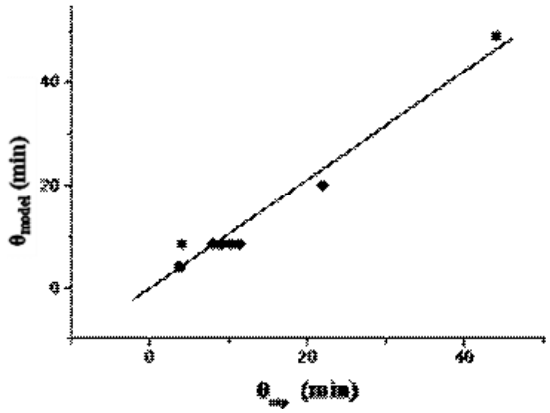

Fig. 9. Induction period for the alkaline decomposition: Comparison between calculated data and experimental data for θ. $Ca(OH)_2 > 2$mM.

$$t_x = [1/[OH^-]^{0.5} \cdot 7.4 \cdot 10^{11} \cdot e^{-71{,}000/RT}] + r_0[1 - (1 - X)^{1/3}] / [(161.3)(59.1) \cdot e^{-42{,}000/RT} \cdot [OH]^{0.5}] \qquad (13)$$

Figure 12 shows the total reaction time for obtaining a conversion of the argentojarosite of x = 0.75, calculated according to expression 13 vs the same parameter, experimentally obtained; we can conclude that expression 13 is consistent with the experimental results.

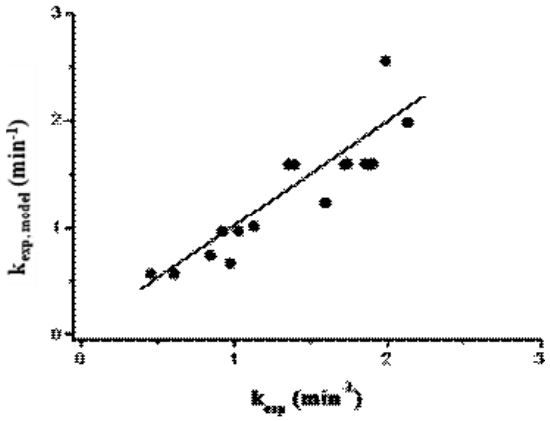

Fig. 10. Conversion period of the alkaline decomposition: Comparison between calculated data and experimental data for k_{exp}. $Ca(OH)_2$ > 2mM.

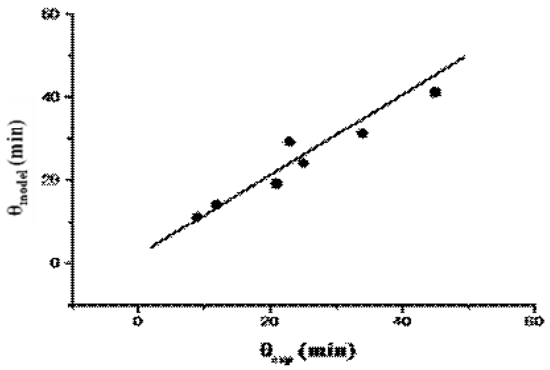

Fig. 11. Induction period for the cyanidation in $Ca(OH)_2$ > 2mM: Comparison between calculated data and experimental data for θ.

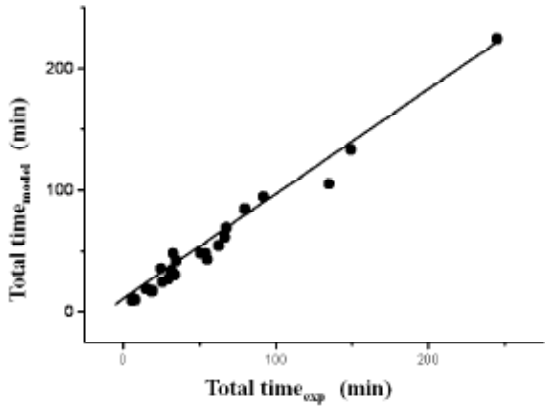

Fig. 12. Alkaline decomposition (NaOH and $Ca(OH)_2$ < 2mM): Chart of the reaction time to obtain a conversion X = 0.75 (calculated vs experimental).

Alkaline decomposition ($Ca(OH)_2$ > 2mM)

For expressions 9 and 10 corresponding to the alkaline decomposition ($Ca(OH)_2$>2mM), an expression is established in order to determine the total reaction time for obtaining a definite conversion of the argentojarosite; the kinetic model is the following:

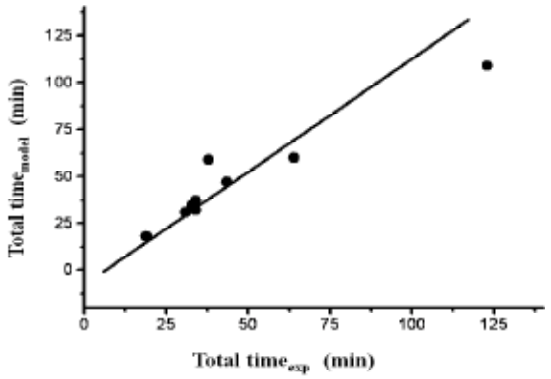

Fig. 13. Alkaline decomposition ($Ca(OH)_2$ > 2mM): Chart of the total reaction time to obtain a conversion X = 0.75 (calculated vs experimental).

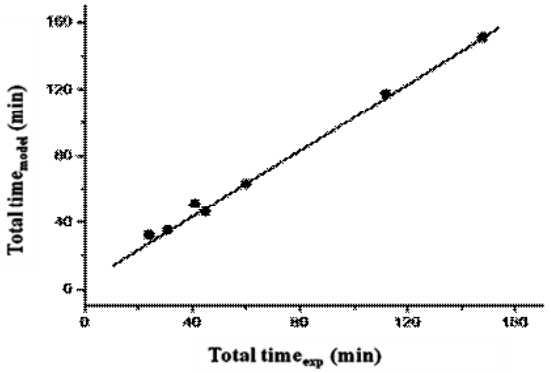

Fig. 14. Cyanidation in $Ca(OH)_2$ > 2mM: Chart of the total reaction time to obtain a conversion of X = 0.75 (calculated vs experimental).

$$t_x = [1/[OH]^0 \cdot 3.6 \cdot 10^{10} \cdot e^{-71{,}000/RT}] + r_0[1 - (1 - X)^{1/3} /[(161.3)(2.34) \cdot e^{-42{,}000/RT} \cdot [OH^-]^0] \quad (14)$$

Figure 13 shows the total reaction time for obtaining a conversion of x = 0.75, calculated according to expression 14 vs the same parameter (experimentally obtained); therefore we can conclude that expression 14 is consistent with the experimental results.

Cyanidation in $Ca(OH)_2$ media

From expressions 11 and 12 we can establish a new expression in order to determine the total reaction time for obtaining a definite dissolution of the silver by cyanidation of the argentojarosite; the kinetic model is the following:

$$t_x = [1/[CN^-]^{0.5} \cdot 3.6 \cdot 10^{10} \cdot e^{-71{,}000/RT}] + r_0[1 - (1 - X)^{1/3}] /[(161.3)(59.1) \cdot e^{-42{,}000/RT} \cdot [OH^0] \cdot [CN^0] \quad (15)$$

Figure 14 shows the total reaction time for obtaining a silver dissolution of X = 0.75, calculated according to expression 15 vs the same (experimentally) obtained parameter; we can conclude that expression 15 is consistent with the experimental results.

Conclusions

The expressions of the global mathematical models for the decomposition of the argentojarosite in the induction period and progressive conversion period in $Ca(OH)_2$ > 2mM, NaOH and $Ca(OH)_2$ < 2mM media, as well as for the cyanidation in $Ca(OH)_2$ > 2mM media are the following:

$$t_x = [1/[OH]^0 \cdot 3.6 \cdot 10^{10} \cdot e^{-71,000/RT}] + r_0[1 - (1 - X)^{1/3} /[(161.3)(2.34) \cdot e^{-42,000/RT} \cdot [OH^-]^0]$$

$$t_x = [1/[OH^-]^{0.5} \cdot 7.4 \cdot 10^{11} \cdot e^{-71,000/RT}] + r_0[1 - (1 - X)^{1/3}] /[(161.3)(59.1) \cdot e^{-42,000/RT} \cdot [OH]^{0.5}]$$

$$t_x = [1/[CN^-]^{0.5} \cdot 3.6 \cdot 10^{10} \cdot e^{-71,000/RT}] + r_0[1 - (1 - X)^{1/3}] /[(161.3)(59.1) \cdot e^{-42,000/RT} \cdot [OH^0] \cdot [CN^0]$$

Experimental

Materials

The argentojarosite used in this work is the one described in previous works [8, 9]. This jarosite whose formula is $Ag_{0.78}(H_3O)_{0.22}Fe_3(SO_4)_2(OH)_6$, has been characterized before [9] and consists of compact spherical aggregates of rhombohedral crystals, which are suitable for the heterogeneous kinetic modeling. Figure 1 shows one of the groups of spherical particles of aggregates used for the kinetic modeling in the alkaline decomposition and cyanidation.

Experimental procedure

The experimental procedure used is similar to that used in previous works [8, 9, 10, 11]. In the alkaline decomposition experiments in NaOH media, we worked under the following conditions: 0.5 g of argentojarosite (38 ± 2 μm and 48 ± 8μm) in an initial volume of 0.5 L at 500 rpm and 30, 50, 60 ^oC, except for the experiments where the different effects were studied. For the experiments in $Ca(OH)_2$ media, 0.5 g of argentojarosite (38 ± 2 μm) were used in an initial volume of 2 L (in order to prevent the saturation of the solution with $CaSO_4$) at 500 rpm and 50 ^oC, except for the experiments where the different effects were studied. For the cyanidation in $Ca(OH)_2$ media 0.5 g of argentojarosite were used under the previously described conditions. The pH was kept constant in both media, adding small amounts of NaOH or $Ca(OH)_2$ solution during experimentation. The OH^- concentration was determined by considering the water ionic product constant and the pH of the alkaline solution according to the working temperatures used in this paper [12].

Monitoring of the decomposition kinetics was carried out by analysis of sulphur using inductively coupled plasma spectrometry (ICP), while the alkaline cyanidation follow-up was carried out by analysis of the silver ion using Atomic Absorption Spectrometry (AAS). For every experiment and every studied effect the induction time (θ) was measured, and the rate experimental constant (k_{exp}) was also determined. With this experimental information the kinetic modeling of the alkaline decomposition and cyanidation of the argentojarosite was carried out. Solids at different times of the alkaline decomposition were analyzed by X-ray diffraction and scanning electron microscopy (SEM) with microanalysis by X-ray energy dispersion (EDS) with the purpose of determining their evolution. Tables 1, 2, 3 and 4 summarize the experimental data obtained, which will be used for the modeling proposed in this work.

Acknowledgements

The authors would like to thank the Consejo Nacional de Ciencia y Tecnología, México, the Universidad Autónoma del Estado de Hidalgo, Hidalgo, México and the Departament d'Enginyeria Química i Metallúrgica, Universitat de Barcelona, Spain.

References

1. Dutrizac, J. E.; Kaiman, S. *Can. Mineral.* **1976**, *14*, 151-158.
2. Dutrizac, J. E.; Jambor, J. L.; O'Reylly, J. B. *CIM Bull*. **1983**, *76*, 78-81.
3. Amorós, J. L.; Lunar, R.; Tavira, P. *Miner. Deposita* **1981**, *16*, 205-213.
4. Dutrizac, J. E.; Jambor, J. L. *Applied Mineralogy,* Park, W. C.; Hausen, D. M.; Hagni, R. D. Eds., AIME, Warrendale, P. A., **1984**, 507-530.
5. Schempp, C. A. *Am. J. Sci*. **1923**, *6*, 73-74.
6. Arregi, Y.; Gordon, A. R.; Steintvelt, S. The Jarosite Process-past, Present and Future. Cigan, J. M.; Mackey, T. S.; O'Keefe, T. J., Eds., *TMS-AIME, New York*, **1979**, 97-123.
7. Salinas, E.; Roca, A.; Cruells, M.; Patiño, F. *Hydrometallurgy* **2001**, *60*, 237-246.
8. Patiño, F. Tesis de doctorado: *Cinética de la cianuración de argentojarosita y sus soluciones sólidas con plumbojarosita*, Universitat de Barcelona, Facultat de Química, España, **1991**.
9. Roca, A.; Patiño, F.; Viñals, J.; Núñez, C. *Hydrometallurgy* **1993**, *33*, 341-358.
10. Cruells, M.; Roca, A.; Patiño, F.; Salinas, E.; Rivera, I. *Hydrometallurgy* **2000**, *55*, 153-163.
11. Patiño, F.; Cruells, M.; Roca, A.; Salinas, E.; Pérez, M. *Hydrometallurgy* **2003**, *70*, 153-162.
12. Lide, D. R. *Handbook of Chemistry and Physics*, 72nd edn, Boston, **1991-1992**, 8-42.
13. Roca, A.; Cruells, M.; Patiño, F.; Rivera, I.; Plata, M. *Hydrometallurgy* **2006**, *81*, 15-23.
14. Ballester, A.; Verdeja, L. F.; Sancho, J., *Metalurgia Extractiva, Vol. 1 Fundamentos,* Editorial Síntesis, Madrid, **2000**, 182-189.
15. Sohn, H. Y.; Wadsworth, M. E., *Cinética de los Procesos de la Metalurgia Extractiva,* Ed. Trillas, México, **1986**, 167-194.
16. Levenspiel, O., *Ingeniería de las Reacciones Químicas,* Editorial Reverté, Barcelona, España, **1979**.